

# Suspended Microchannel Resonators for Ultralow Volume Universal Detection

Sungmin Son,<sup>†</sup> William H. Grover,<sup>‡</sup> Thomas P. Burg,<sup>‡</sup> and Scott R. Manalis<sup>\*,†,‡</sup>

Department of Mechanical Engineering, and Department of Biological Engineering, Massachusetts Institute of Technology, Cambridge, Massachusetts 02139

Universal detectors that maintain high sensitivity as the detection volume is reduced to the subnanoliter scale can enhance the utility of miniaturized total analysis systems ( $\mu$ -TAS). Here the unique scaling properties of the suspended microchannel resonator (SMR) are exploited to show universal detection in a 10 pL analysis volume with a density detection limit of  $\sim 1 \mu\text{g}/\text{cm}^3$  (10 Hz bandwidth) and a dynamic range of 6 decades. Analytes with low UV extinction coefficients such as polyethylene glycol (PEG) 8 kDa, glucose, and glycine are measured with molar detection limits of 0.66, 13.5, and  $31.6 \mu\text{M}$ , respectively. To demonstrate the potential for real-time monitoring, gel filtration chromatography was used to separate different molecular weights of PEG as the SMR acquired a chromatogram by measuring the eluate density. This work suggests that the SMR could offer a simple and sensitive universal detector for various separation systems from liquid chromatography to capillary electrophoresis. Moreover, since the SMR is itself a microfluidic channel, it can be directly integrated into  $\mu$ -TAS without compromising overall performance.

Among the various detection methods for high-performance liquid chromatography (HPLC),<sup>1</sup> universal detectors provide an important alternative to the commonly used UV–vis detectors as they can analyze chemicals without chromophores or fluorophores.<sup>2</sup> For example, evaporative light scattering detectors (ELSD) have been used to detect nonvolatile compounds such as lipids,<sup>3</sup> carbohydrates,<sup>4</sup> and pharmaceutical compounds,<sup>5,6</sup> which exhibit weak optical absorbance in the UV–vis region. However, ELSD is considered a semiuniversal detector because the sensitivity depends strongly on the volatility of the analytes

and mobile phases.<sup>7</sup> The refractive index detector (RID), which is the most widely used universal detector,<sup>8</sup> responds to essentially all analytes<sup>9</sup> without requiring modification of the sample. State-of-the-art commercial RIDs achieve detection limits on the order of  $10^{-9}$  refractive index units (RIU) for volumes on the microliter scale.<sup>10</sup> For samples where the signal-to-noise of the differential mass density is greater than the differential refractive index,<sup>11</sup> densitometry can be used in place of RID to improve sensitivity. For example, Trathnigg and Jorde used an oscillating glass capillary tube to measure density with a detection limit of  $0.35 \mu\text{g}/\text{cm}^3$  in a volume of  $20 \mu\text{L}$ . For glycine, such a detection limit is roughly equivalent to  $2 \times 10^{-11}$  RIU, which is nearly 100-fold more sensitive than the commercial RID.

Proliferation of miniaturized analysis techniques such as micro-high-performance liquid chromatography ( $\mu$ HPLC) and capillary electrophoresis (CE) has led to the necessity of on-column<sup>12</sup> analysis of solutes in nanoliter to picoliter volumes with high sensitivity and in the absence of derivatization chemistry.<sup>13,14</sup> As UV absorption does not scale favorably due to path length dependency<sup>12,15</sup> and nonlinear response to sample concentration,<sup>16</sup> effort is being directed toward maintaining high sensitivity with RID while scaling the detection volume down to the nanoliter regime. For example, Wang and Bornhop developed dual-capillary dual-bicell microinterferometric backscattering detection<sup>17</sup> that achieved a sensitivity of  $10^{-9}$  RIU in a 50 nL detection volume. As an extension of this work, Bornhop et al. achieved a detection limit of  $10^{-6}$  RIU in a 350 pL volume with a simple and elegant approach that required only a helium–neon laser, a microfluidic channel, and a position sensor.<sup>18</sup> Effort is also being directed toward developing miniaturized densitometers. Corman et al. demonstrated a detection limit of  $4 \mu\text{g}/\text{cm}^3$  in a  $35 \mu\text{L}$  volume

\* To whom correspondence should be addressed. Phone: +1 617-253-5039. Fax: +1 617-253-5102. E-mail: scottm@media.mit.edu.

<sup>†</sup> Department of Mechanical Engineering.

<sup>‡</sup> Department of Biological Engineering.

- (1) Yeung, E. S., Ed. *Detectors for Liquid Chromatography*, Chemical Analysis 89; Wiley: New York, 1986.
- (2) Weston, A.; Brown, P. R. *HPLC and CE: Principles and Practice*, 1st ed.; Academic Press: London, 1997.
- (3) Moreau, R. A.; Powell, M. J.; Hicks, K. B. *J. Agric. Food Chem.* **1996**, *44*, 2149–2154.
- (4) Wei, Y.; Ding, M. Y. *J. Chromatogr., A* **2000**, *904*, 113–117.
- (5) Asmus, P. A.; Landis, J. B. *J. Chromatogr.* **1984**, *316*, 461–472.
- (6) Strege, M. A.; Stevenson, S.; Lawrence, S. M. *Anal. Chem.* **2000**, *72*, 4629–4633.

(7) Scott, R. P. W. In *Analytical Instrumentation Handbook*; Ewing, G. W., Ed.; Marcel Dekker: New York, 1997; pp 1123–1203.

(8) Ravindranath, B. *Principles and Practice of Chromatography*; Halsted Press: New York, 1989.

(9) Wang, Z.; Bornhop, D. J. *Anal. Chem.* **2005**, *77*, 7872–7877.

(10) Thermo Electron Corporation. Product Specifications, 2003.

(11) Trathnigg, B.; Jorde, C. J. *Chromatogr.* **1987**, *385*, 17–23.

(12) Yang, F. J. *High Resolut. Chromatogr. Chromatogr. Commun.* **1981**, *4*, 83.

(13) Markov, D. A.; Swinney, K.; Bornhop, D. J. *J. Am. Chem. Soc.* **2004**, *126*, 16659–16664.

(14) Swinney, K.; Pennington, J.; Bornhop, D. J. *Microchem. J.* **1999**, *62*, 154–163.

(15) Bruno, A. E.; Paulus, A.; Bornhop, D. J. *J. Appl. Spectrosc.* **1991**, *45*, 462–467.

(16) Bruno, A. E.; Krattiger, B.; Maystre, F.; Widmer, H. M. *Anal. Chem.* **1991**, *63*, 2689–2697.

(17) Wang, Z.; Bornhop, D. J. *Anal. Chem.* **2005**, *77*, 7872–7877.

(18) Bornhop, D. J.; Latham, J. C.; Kussrow, A.; Markov, D. A.; Jones, R. D.; Sorensen, H. S. *Science* **2007**, *317*, 1732–1736.

with a low-pressure encapsulated silicon densitometer with integrated feedback control electronics,<sup>19</sup> and Sparks et al. used a related approach to achieve a detection limit of  $28 \mu\text{g}/\text{cm}^3$  in a  $0.6 \mu\text{L}$  volume.<sup>20</sup> These results, in light of those by Trathnigg and Jorde, indicate that densitometers can maintain high sensitivity as the analysis volume is reduced.

In this paper, we show that the suspended microchannel resonator (SMR) can be used as a universal detector to resolve relative density changes of  $1 \mu\text{g}/\text{cm}^3$  within a volume of  $10 \text{ pL}$ . The SMR differs from the aforementioned densitometers both in terms of scale and sensitivity: the combination of the low resonator mass ( $100 \text{ ng}$ ) and high quality factor ( $15\,000$ ) enables a minimum detectable mass of approximately  $1 \text{ fg}$ .<sup>21</sup> To demonstrate the utility of the SMR for real-time detection, we have coupled it to HPLC and measured the response from various analytes introduced by liquid mobile phases. We discuss the analytical attributes of linearity, dynamic range, sensitivity, and noise considerations, and we present a comparison between the HPLC-SMR and conventional HPLC-UV-vis. Since the SMR is manufactured by conventional semiconductor fabrication processes, it can ultimately be integrated with upstream microfluidic sample preparation and separation stages to create a miniaturized total analysis system ( $\mu\text{-TAS}$ ).

## EXPERIMENTAL SECTION

**Chemicals.** Polyethylene glycols (PEG) 4, 8, and  $20 \text{ kDa}$  were purchased from Sigma Chemical Co. (St. Louis, MO);  $1$  and  $31 \text{ kDa}$  were from Polymer Laboratories (Shropshire, U.K.). L-Glucose, glycine, and bovine serum albumin (BSA) were obtained from Sigma Chemical Co. (St. Louis, MO). All solutions were prepared with water purified by a Millipore Simplicity system (Millipore, Bedford, MA).

**Experimental Setup.** A description of the SMR device and its operation has been previously published.<sup>21</sup> For the device used in this work, the density sensitivity of  $10\,470 \text{ Hz}/(\text{g cm}^{-3})$  was measured by using solvents of known density such as water, acetonitrile, and toluene.

The HPLC system consisted of an Agilent 1100 HPLC system (Agilent Technologies, Palo Alto, CA) including a binary LC pump, micro autosampler with a six-port switching valve equipped with a loop volume of  $40 \mu\text{L}$ , and a multiwavelength detector (MWD) with an  $80 \text{ nL}$ ,  $6 \text{ mm}$  path length flow cell. Microflow mode with a  $100 \mu\text{L}/\text{min}$  maximum was used to precisely adjust the flow rate of the mobile phase for the flow injection analysis and gel filtration chromatography (GFC). Sample injection and flow adjustment were entirely automated. A Tosoh Bioscience SuperSW3000 gel filtration column ( $30 \text{ cm}$  length,  $2 \text{ mm}$  i.d.,  $4 \mu\text{m}$  particle size,  $500\,000 \text{ Da}$  pore size) was used without a guard column.

Figure 1a shows a schematic diagram of the HPLC-SMR apparatus. A  $5 \text{ cm}$  length of PEEK tubing ( $1/32 \text{ in. o.d.} \times 0.010 \text{ in. i.d.}$ ) was used to connect the injector valve to the separation column. The eluate was sent to either the SMR or the MWD. A  $12 \text{ cm}$  length of PEEK tubing ( $1/32 \text{ in. o.d.} \times 0.0025 \text{ in. i.d.}$ ) was used to connect the column to the MWD. A  $20 \text{ cm}$  length of FEP

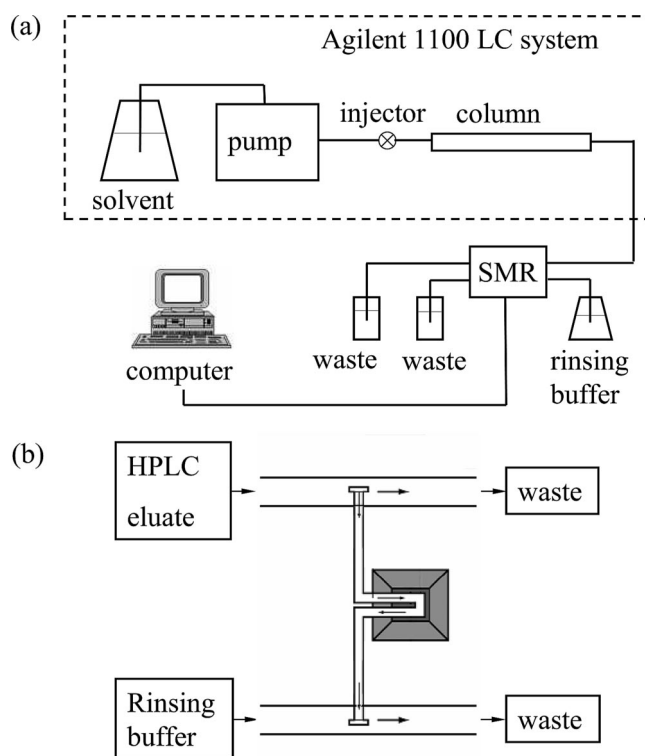


**Figure 1.** (a) Flow diagram of the suspended microchannel resonator (SMR) detection system. Solution leaving the column enters a small-volume ( $10 \text{ pL}$ ) suspended microchannel (b) which reports on the density of the eluate. The density monitored as a function of separation time produces a chromatogram. Since the flow cross section of the suspended microchannel is about 70 times smaller than that of the bypass channels, only  $\sim 1/3000$  of the bypass flow is directed into the suspended microchannel. The linear flow rate through the suspended microchannel is  $\sim 13 \text{ mm/s}$  when the volumetric flow rate through the column is  $65 \mu\text{L}/\text{min}$ .

tubing ( $1/32 \text{ in. o.d.} \times 0.003 \text{ in. i.d.}$ ) was used to connect the column to the SMR. For flow injection analysis, a  $30 \text{ cm}$  length of PEEK tubing ( $1/32 \text{ in. o.d.} \times 0.010 \text{ in. i.d.}$ ) was used along with a microtight union (Upchurch Scientific) to connect the injector valve to either the SMR or MWD instead of the column.

Figure 1b shows the flow path in the bypass channels and the suspended microchannel of the device. Two  $10 \text{ nL}$  bypass channels were needed to decrease the flow resistance and accommodate the flow rate of  $65 \mu\text{L}/\text{min}$ , which is optimal for GFC. Although most of the HPLC eluate flows out to the waste reservoir of the upper bypass channel, a small portion flows through the suspended microchannel. The flow rate through the suspended microchannel is determined by the pressure difference between its inlet and outlet. Since the flow cross section of the suspended microchannel is about 70 times smaller than that of the bypass channels, the linear flow rate can be much faster in the suspended microchannel than in the bypass channel, even though the pressure difference across the suspended microchannel is small. Therefore, at any given time, it is assumed that the SMR is measuring the eluate that is present at the inlet of the suspended microchannel. For a flow rate of  $65 \mu\text{L}/\text{min}$  in one bypass channel and a pressure of  $\sim 6 \text{ psi}$  in the inlet of the other bypass channel regulated using precision pressure regulators (Omega Engineering, PRG101-25), the pressure difference across the suspended

(19) Corman, T.; Enoksson, P.; Noren, K.; Stemme, G. *Meas. Sci. Technol.* **2000**, *11*, 205–211.

(20) Sparks, D.; Smith, R.; Straayer, M.; Cripe, J.; Schneider, R.; Chimbayo, A.; Anasari, S.; Najafi, N. *Lab Chip* **2003**, *3*, 19–21.

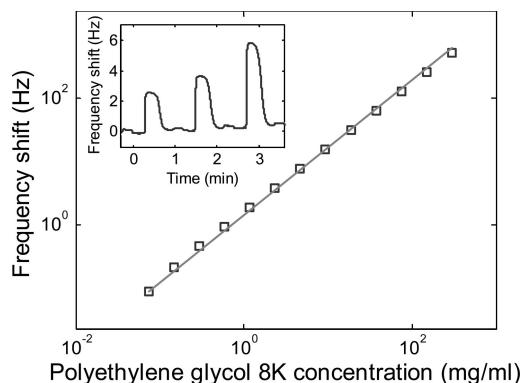


**Figure 2.** Various concentrations of PEG 8 kDa were measured from the most dilute to the most concentrated with a 15  $\mu\text{L}/\text{min}$  flow rate and without the column. The inset shows the SMR time response to three different concentrations of PEG (0.59, 1.2, and 2.3 mg/mL each). The relative height of the peak from the baseline was used to determine each point of the frequency–concentration curve.

microchannel was  $\sim 10$  psi, leading to the linear flow rate of 13 mm/s through the suspended microchannel.

**Detection Schemes.** The  $\sim 200$  kHz mechanical resonant frequency of the SMR is mixed down with a reference oscillator whose frequency is  $\sim 1$  kHz below the resonant frequency. The down-converted signal is then rectified and measured with the time–frequency counter (National Instruments PCI-MIO-16 multifunctional DAQ card). With this scheme, the data acquisition rate is dictated by the frequency of the mixed-down signal ( $\sim 1$  kHz). Noise is reduced off-line using a Savitzky–Golay filter and a moving average filter, resulting in a final sampling rate of 10 Hz.

## RESULTS AND DISCUSSION

**Dynamic Range and Limit of Detection.** The linearity of the SMR was determined by injecting 30  $\mu\text{L}$  sample plugs of 8 kDa PEG without a column at concentrations ranging from 0.1 mg/mL to its maximum solubility of  $\sim 300$  mg/mL (Figure 2). The inset of Figure 2 shows the SMR frequency response to the saturated peak versus time for three different concentrations of PEG. Baseline instability between peaks was primarily due to pressure variations across the SMR created by the sample exchange valve. As a control, only the mobile phase (water) was injected following each PEG sample, and a reproducible peak response that was independent of the sample concentration was routinely observed. This offset was attributed to nonspecific contamination entering the SMR from the HPLC fluid path. To accommodate for this offset, the response from the mobile phase was subtracted from each sample response.

To determine the SMR detection limit, the baseline signal was acquired over a 90 s period with a 10 Hz sampling rate as the water eluted from a gel filtration column was driven through the bypass channel at a flow rate of 65  $\mu\text{L}/\text{min}$ . The three standard deviation ( $3\sigma$ ) of the resulting signal was found to be 9.6 mHz. The concentration sensitivity of the SMR was on the order of 0.1  $\mu\text{g}/(\text{mL mHz})$  but differed slightly depending on the particular sample. That is, the detection limit resulting from sensitivities measured for glycine and glucose was approximately 2.5  $\mu\text{g}/\text{mL}$ , and for 8 kDa PEG and BSA it was approximately 5.5  $\mu\text{g}/\text{mL}$ . These values lead to the molar detection limit of 0.085  $\mu\text{M}$  for

**Table 1. Typical Properties of the SMR and Other Common HPLC Detectors**

	ELSD <sup>a</sup>	UV–vis <sup>b</sup>	RID <sup>c</sup>	SMR
analyte response	mass/volatility	optical absorbance	refractive index	mass
LOD for glycine <sup>d</sup>	5 $\mu\text{g}/\text{mL}$	2 $\mu\text{g}/\text{mL}$	50 $\mu\text{g}/\text{mL}$	2.5 $\mu\text{g}/\text{mL}$
linear range	$10^1$ – $10^3$	$10^4$ – $10^5$	$10^5$	$10^6$
universal	semi	no	yes	yes

<sup>a</sup> Sedex 55, Sedex (Vitry-sur-Seine, France). <sup>b</sup> L-2400, Merck-Hitachi (Merck, Darmstadt, Germany). <sup>c</sup> SpectraSYSTEM RI-150, Thermo Separation Product (Les Ulis, France). <sup>d</sup> Ref 24.

BSA, 0.66  $\mu\text{M}$  for 8 kDa PEG, 13.5  $\mu\text{M}$  for glucose, and 31.6  $\mu\text{M}$  for glycine. Considering the detection limit of 0.97 nM for BSA obtained by absorbance at 220 nm, UV–vis absorbance is nearly 100-fold more sensitive than the SMR for samples with high extinction coefficients and detectors with sufficiently long optical path lengths. However, the SMR detector is more sensitive than RID. As shown in Table 1, in the case of weakly UV absorbing samples such as glycine, the SMR can resolve a concentration of  $\sim 2.5$   $\mu\text{g}/\text{mL}$  in a 10 pL volume, whereas the commercial RID<sup>10</sup> resolves  $\sim 50$   $\mu\text{g}/\text{mL}$  in an 8  $\mu\text{L}$  volume. An important aspect of detection by fluid density using the SMR is the wide dynamic range offered by the method. Although the frequency noise of 3.2 mHz (10 Hz bandwidth) dictates the limit of detection for low concentrations, frequency changes as large as 10 kHz can be reliably measured. For example, a frequency shift of 10 800 Hz results upon priming an air-filled cantilever with pure water. The dynamic range of the measurement therefore exceeds 6 orders of magnitude, with a maximum systematic deviation from linearity of 7.5% due to the nonlinear relationship between resonance frequency and mass.

**Chromatogram.** To demonstrate that SMR detection can be used for real-time eluate monitoring, a chromatogram was acquired from a GFC separation. A 3  $\mu\text{L}$  sample of a PEG mixture containing various molecular weights (1, 4, 8, 20, and 31 kDa; 5 mg/mL each) was injected at a flow rate of 65  $\mu\text{L}/\text{min}$  in a mobile phase of purified water. To validate the SMR response, a chromatogram was also acquired by measuring the UV–vis absorbance of the eluate at a wavelength of 196 nm (4 nm bandwidth and slit width). As shown in Figure 3, the retention time, peak width, and resolution are well-matched in both chromatograms.

The short-term instability of the SMR baseline was primarily due to variations in pressure. For example, the peak at  $t \sim 0.3$  min was due to a pressure increase induced by switching the injection valve from the loading to running position. Even though large pressure changes during elution are not expected, the viscosity differences within the eluted sample effectively alter the pressure and induce signal artifacts. In addition, the active flow rate control of the HPLC pump can cause periodic pressure changes which can be observed from the SMR signal as well. However, these variations can be compensated for off-line by calibrating the frequency–pressure relationship. Alternatively, using another elution mechanism such as electrokinetic separation could avoid this problem. The long-term drift (approximately 100 mHz over 10 min) was primarily due to drift in ambient temperature. We anticipate that this drift could

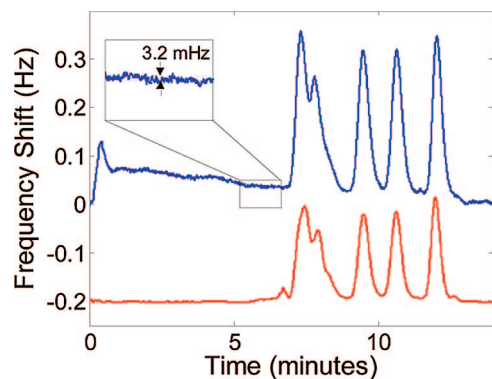


**Figure 3.** Chromatograms resulting from the HPLC separation and SMR (top) or UV-vis (bottom) detection of a five-component mixture of PEGs (31, 20, 8, 4, and 1 kDa in order eluted). In the inset, the baseline noise of the SMR for 90 s shows the standard deviation of 3.2 mHz. The UV-vis chromatogram was offset vertically from the SMR chromatogram for clarity (1 Hz equal to 250 mAU in UV-vis).

be eliminated by either using temperature control or making a differential measurement with an adjacent SMR sensor.<sup>21</sup>

## CONCLUSIONS

We have demonstrated that the SMR can be used for real-time universal detection. When compared to a state-of-the-art commercial RID system,<sup>10</sup> the SMR achieves a more than 10-fold improvement in detection limit (as determined with glycine) for an analysis volume that is  $10^5$ -fold smaller. Since the SMR is a batch-fabricated microfluidic device, it can be readily integrated

within  $\mu$ -TAS without compromising overall performance.<sup>22</sup> The device used throughout this work is already compatible with the volumes and flow rates typically available in microfluidics, and with appropriate integration, similar results should be attainable in the context of detection in  $\mu$ -TAS. Moreover, the detection limit of the SMR as determined by the thermomechanical noise is approximately 4 ng/cm<sup>3</sup>, and we anticipate that optimization of the frequency detection circuitry will ultimately allow us to approach this limit.

We envision that the SMR's ability to detect the binding of specific molecules to its interior surface could enable immunoaffinity CE (IACE) applications.<sup>23</sup> We recently showed that, using a monolayer coverage (2 pmol cm<sup>-2</sup>) of active antibodies with a dissociation constant of 1 nM, the SMR can detect the binding of a 30 kDa analyte with a detection limit on the order of 1 pM.<sup>21</sup> For multianalyte detection, arrays of SMRs could be functionalized with different capture molecules.

## ACKNOWLEDGMENT

We thank Ken Babcock for valuable discussions, and we acknowledge financial support from the National Institutes of Health (NIH) Grant EB003403 and the National Institute of General Medical Sciences (NIGMS) Cell Decision Process Center Grant P50-GM68762.

Received for review February 13, 2008. Accepted April 14, 2008.

AC800307A

(21) Burg, T. P.; Godin, M.; Knudsen, S. M.; Shen, W.; Carlson, G.; Foster, J. S.; Babcock, K.; Manalis, S. R. *Nature* **2007**, *446*, 1066–1069.

(22) Burg, T. P.; Manalis, S. R. *J. Microelectromech. Syst.* **2006**, *15*, 1466–1476.

(23) Guzman, N. A. *Anal. Bioanal. Chem.* **2004**, *378*, 37–39.

(24) Petritis, K.; Elfakir, C.; Dreux, M. *J. Chromatogr., A* **2002**, *961*, 9–21.